Fountain and Upwash Flowfields of Multijet Arrangements

F. A. Wohllebe* and M. J. Siclari†
Grumman Aerospace Corporation, Bethpage, N. Y.

A series of cold-gas experiments was performed to determine the characteristics of the upwash and fountain regions of multijets exhausting normal to a ground plane. Detailed total pressure surveys were taken in lateral and vertical planes for both two-jet upwash and three-jet fountain flows. Fountain measurements are presented which depict the gradual formation of coalescent fountain flow from its constituent two-jet upwash flows. Flow visualizations of the ground and vertical planes of symmetry are presented for three-jet fountain flow. Stagnation line behavior under conditions of asymmetry were achieved by rotating the ground plane. Comparisons with a semiempirical prediction methodology are also presented.

Nomenclature

d = nozzle exit diameter
e = distance between centers of two jets
h = height of nozzle exit above ground plane
NPR = nozzle exit pressure ratio $= P_{t_j}/P_A$
ΔP_t $= P_t - P_A$
$\overline{\Delta P_t}$ $= (P_t - P_A)/(P_{t_{j1}} - P_A)$
P = pressure
r = radial distance from jet centerline
x = longitudinal coordinate perpendicular to plane containing two nozzle centerlines (see Fig. 1)
y = lateral coordinate parallel to plane containing two nozzle centerlines (see Fig. 1)
z = vertical coordinate above ground plane
θ = pitch angle, measured in plane symmetry of three-jet arrangement (pitch angle changed by rotating nozzle assembly as a unit)
ϕ = roll angle, measured in plane perpendicular to plane of symmetry of three-jet arrangement (roll angle changed by rotating ground plane)

Subscripts

A = ambient
j = jet exit
m = maximum
0 = reference
t = total
1,2,3 = relating to jet numbers 1,2, or 3 from Fig. 1

Introduction

RECENT developments in analytical methodology[1-3] to predict the fountain and upwash characteristics of multijet VTOL aircraft have shown the need for substantiating experimental data. With this need in mind, several experiments were conducted to obtain the local total pressure distribution in the upwash and fountain flowfield regions of two- and three-jet nozzles exhausting normal to a ground plane. A baseline three-jet array was selected with sufficiently wide spacing to assure reasonable development of constituent parts of the flowfield and stability of the fountain upwash regions.

Figure 1 shows the jet arrangement and vertical survey planes used in various experiments. The front jet (No. 2) was purposely weakened to operate at a nozzle exit pressure ratio (NPR) of 1.29, while the two rear jets (Nos. 1 and 3) were operated at an NPR of about 1.40. This assured that the central fountain would fall completely within the inner region of the three-jet array. Nozzle exits were set sufficiently high ($Z_j/d = 5.6$ to 8.0) so that a significant number of survey passes could be made above the transition region. Survey probe position relative to the jet nozzles is shown in the test setup photo, Fig. 2.

Two-jet surveys were conducted by deactivating nozzle No. 2 for jets of equal strength, or by deactivating nozzle No. 3 to obtain a pair of unequal jets. Aside from the pressure probe, all surveys were conducted without an interfering surface between jet nozzles. Detailed flowfield pressure measurements of the upwash and fountain regions were made using a Kiel probe mounted on an electromechanical traverse device. A precision potentiometer attached to the traverse arm was used to automatically measure and record probe position in the flowfield. Probe pressures were converted to electrical signals with a pressure transducer and were simultaneously recorded with probe position.

A characteristic of the Kiel probe is that it need not be accurately aligned with the local flow direction to measure total pressure. The probe yields the correct pressure for a flow angle range of at least ± 30 deg. To obtain reasonable probe alignment with the local flow direction, a wool tuft was initially passed through the flowfield and the probe aligned accordingly.

Although all pressure measurements were made with jet impingement normal to the ground plane, several flow visualization photos are presented where impingement is at a roll or pitch angle. Some of the resulting ground stagnation lines together with normal impingement upwash pressures are compared with calculated results using methodology developed in Ref. 1.

Two-Jet Upwash

Typical upwash total pressure profiles for two equal jets are shown in Fig. 3. Since downstream conditions can be affected by conditions at the jet exits, nozzle exit pressure profiles were also determined at a distance of $0.57d$ below each exit. The relatively uniform jet exit pressure profile shown by the inset on Fig. 3 is typical of all test results reported herein.

In order to compare decay rates and pressure profile shapes with results calculated by the methods of Ref. 1, upwash profiles were nondimensionalized with peak total pressure at an initial height as shown in Fig. 4. Calculated results use jet impingement points as a virtual decay origin. Predicted decay rates are in fair agreement with measured values. Profile shapes also show reasonable agreement except in regions of near ambient total pressure. Here, the measured results depart

Received Dec. 20, 1977; revision received April 17, 1978.

Index categories: Aerodynamics; Jets, Wakes, and Viscid-Invscid Flow Interactions; Subsonic Flow.

*Aerodynamic Group Specialist. Member AIAA.
†Research Scientist. Member AIAA.

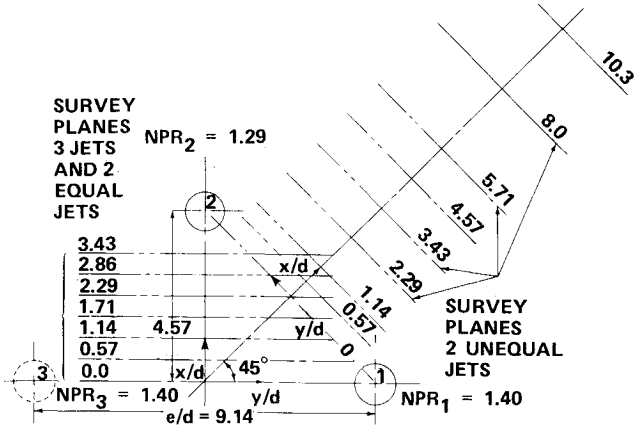

Fig. 1 Relationship of jet locations and survey planes.

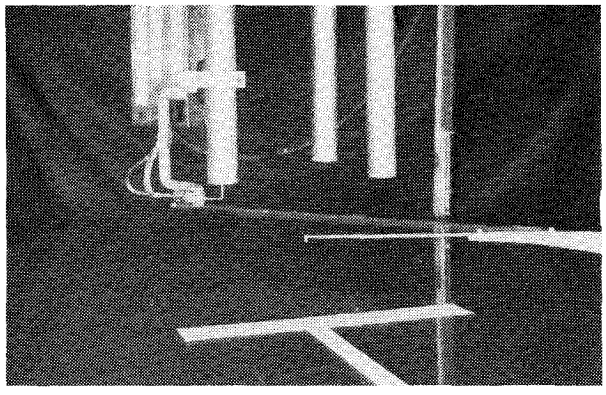

Fig. 2 Kiel total pressure probe beneath three-jet test arrangement.

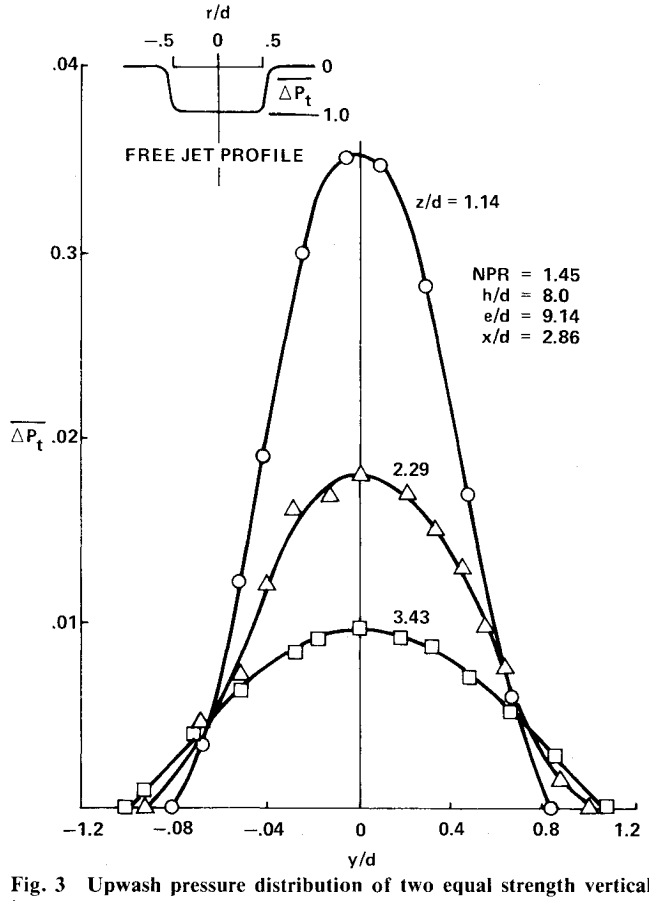

Fig. 3 Upwash pressure distribution of two equal strength vertical jets.

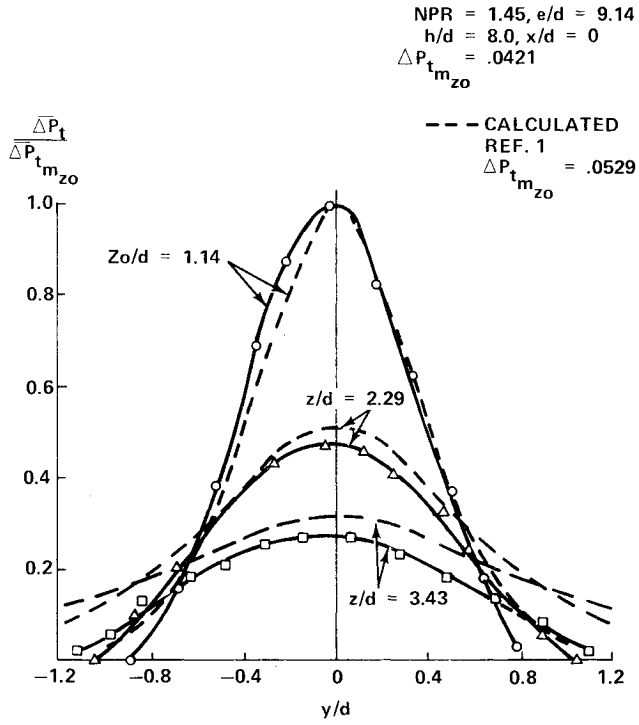

Fig. 4 Comparison of calculated and experimental upwash pressure distributions, two equal jets.

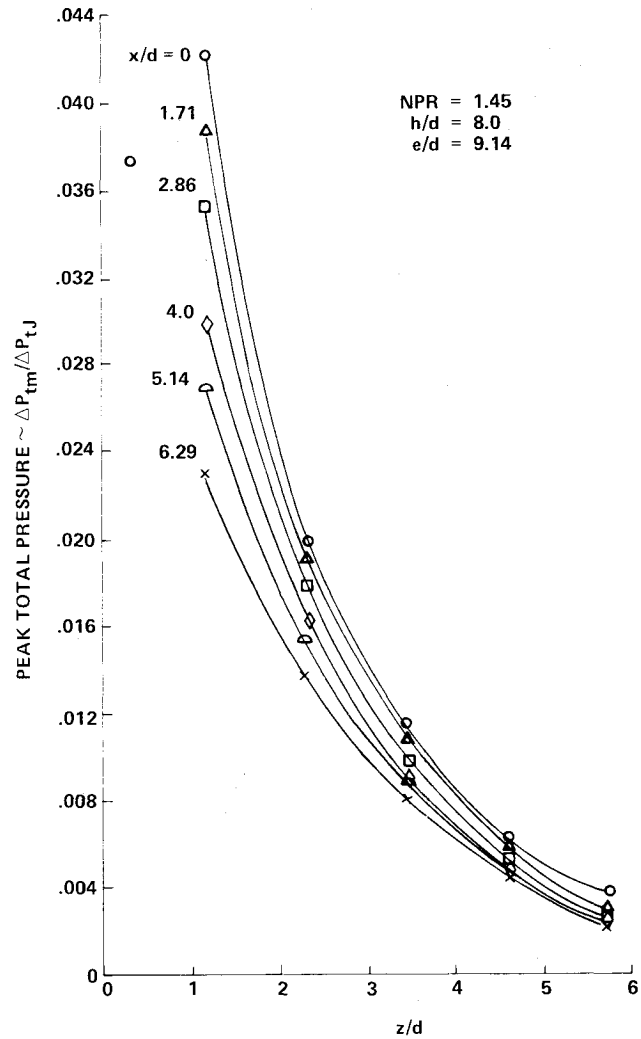

Fig. 5 Peak total pressure decay in the upwash of two equal jets.

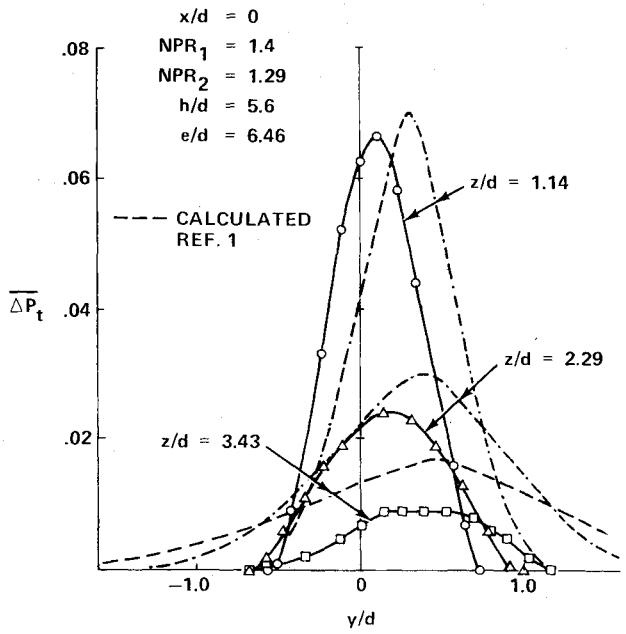

Fig. 6 Measured and calculated upwash pressure distributions, two unequal jets.

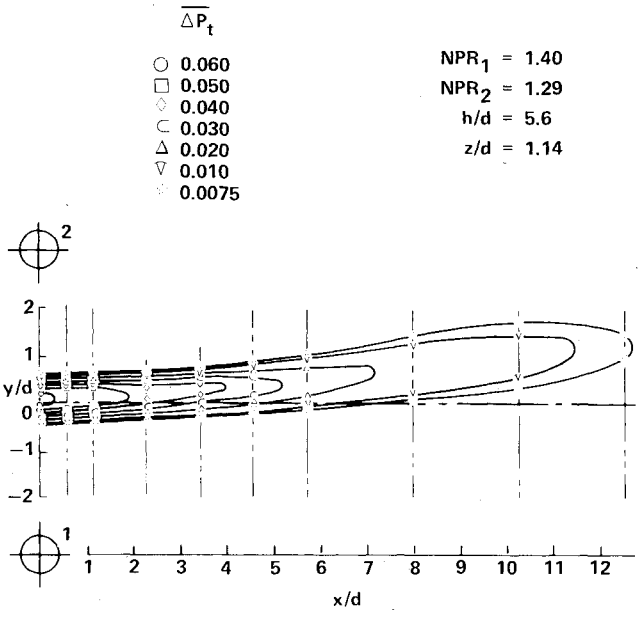

Fig. 7 Isopressure distribution in the upwash of two unequal jets.

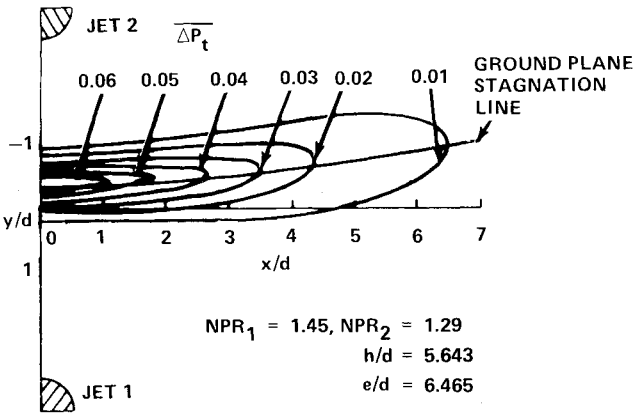

Fig. 8 Predicted isopressure distribution in the upwash of two unequal jets, $Z/d = 1.14$.

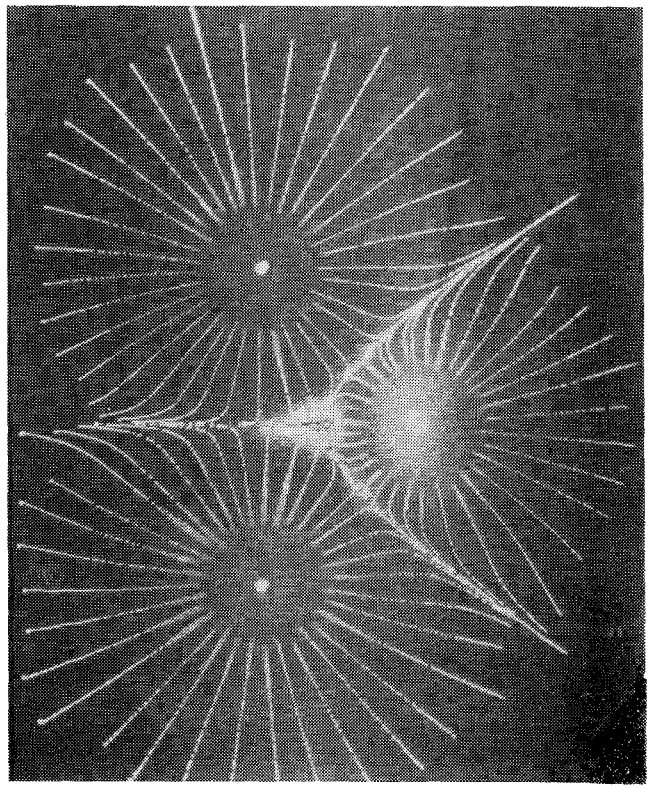

Fig. 9 Ground flow visualization of three-jet configuration with $\theta = 2$ deg, 40 min.

from a free shear profile by decreasing rapidly toward zero with little or no inflection. This behavior was found to be typical of all upwash flows and suggests the presence of a flow recirculation between the jet and the upwash primary flow. Peak total pressure in the upwash field decreases very rapidly with increasing height above ground. Figure 5 illustrates this rapid decay for the entire survey field.

When the test setup is altered to give two jets of unequal NPR, the resulting upwash pressure profiles are shifted toward the weaker jet as shown in Fig. 6. The progressive displacement of peak pressures as survey height above ground increases suggests that the upwash is also inclined toward the weaker jet. For the NPR's tested, the inclination is about 4 deg. This contrasts with the modeling assumption in Ref. 3 that the upwash remains perpendicular to the ground plane. The assumption is probably adequate if the difference in NPR between nozzle pairs is not too great.

Figure 6 also compares test data with calculated results using Ref. 1 methodology. Generally, both the calculated shape and decay rate of the pressure profiles show reasonable agreement with tests. The apparent displacement of the calculated profile, evident at the lowest height, indicates that the intial trajectory or origin of the upwash in the deflection region was not properly taken into account. Subsequent iterations, based on available experimental data, would bring about better agreement.

The isopressure distribution for two unequal jets in a plane parallel to the ground at a height, $Z/d = 1.14$, is shown in Fig. 7. At this low height, the upwash field is narrow and quite well defined. A comparable computed isopressure distribution is shown in Fig. 8. Although the patterns are generally similar, the calculated isopressure distribution shows too rapid a pressure decay in the X direction.

Three-Jet Stagnation Lines, Fountain Location

Oil streak patterns can be very useful in visualizing the complex flowfield that occurs when multiple jets interact with a ground plane. Figure 9 is a ground plane flow visualization

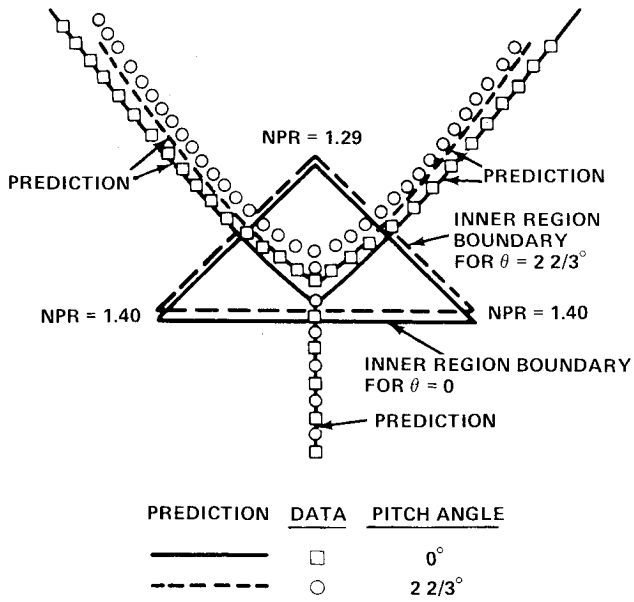

Fig. 10 Three-jet stagnation line prediction and experimental results.

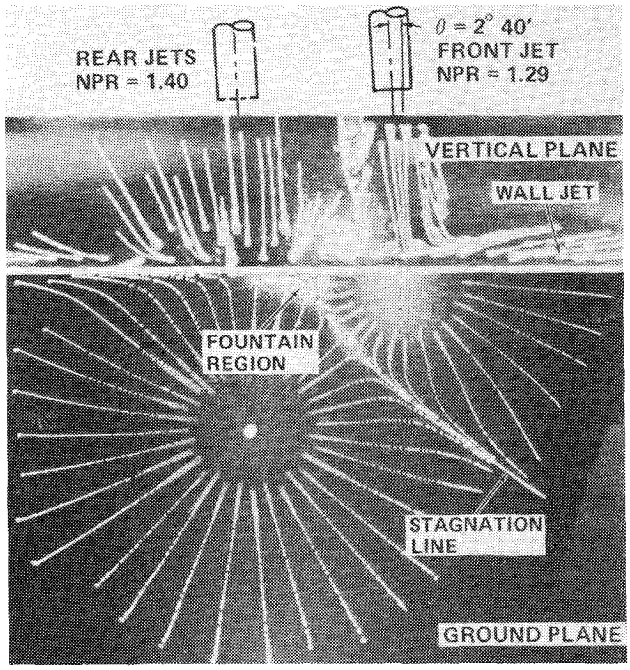

Fig. 11 Ground plane and vertical plane composite flow visualization.

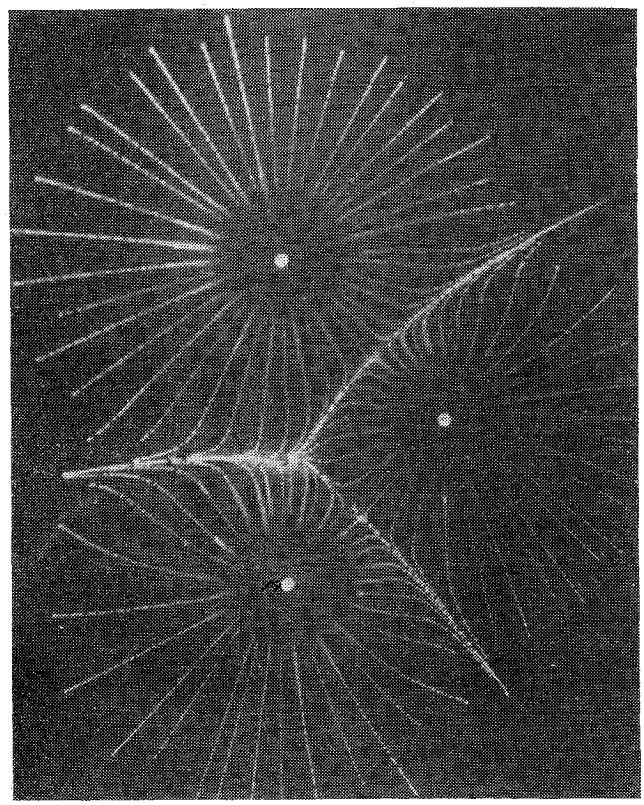

Fig. 12 Ground plane flow visualization of three-jet configuration with $\phi = 10$ deg.

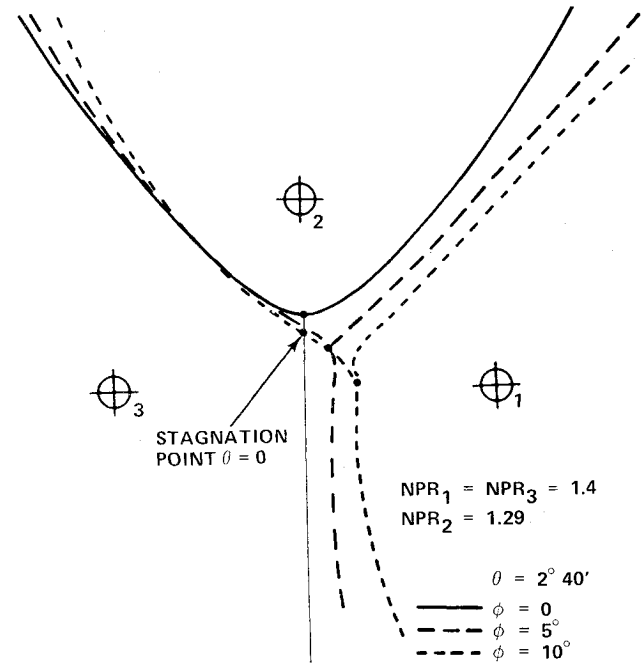

Fig. 13 Effect of roll and pitch attitude on three-jet stagnation lines.

of the reference three-jet nozzle arrangement with a 2-deg, 40-min pitch attitude. The central fountain region is clearly visible at the intersection of three stagnation lines. Another distinctive feature which can be seen is the deposit of flow visualization fluid in the impingement region of the weaker front jet. This suggests that a recirculation occurs near the front jet.

Calculated and experimental stagnation line locations are compared in Fig. 10 for two pitch attitude conditions. The experimental stagnation line patterns indicate that the fountain lies closer to jet No. 2 than predicted by theory. This difference is explained by another experiment where a thin vertical plate in the plane of symmetry was used to generate a cross section of the vertical flow pattern. A composite view of both ground plane and vertical plate flow visualizations is shown in Fig. 11. This flow pattern indicates the formation of a distinct vortex and recirculation region between the fountain and jet No. 2. The fountain flow, which appears to be initially inclined, is turned upward and a boundary forms between it and the induced flow around jet No. 2. The flow visualization fluid on the jet side of the boundary is initally induced downward by the freejet and then is rapidly turned upward. Some of the entrained flow is also drawn into a vortex that appears to have an axis that roughly parallels the front stagnation line. The formation of this vortex probably affects the location of the adjacent stagnation line and may account for the disparity between calculated results and experiments.

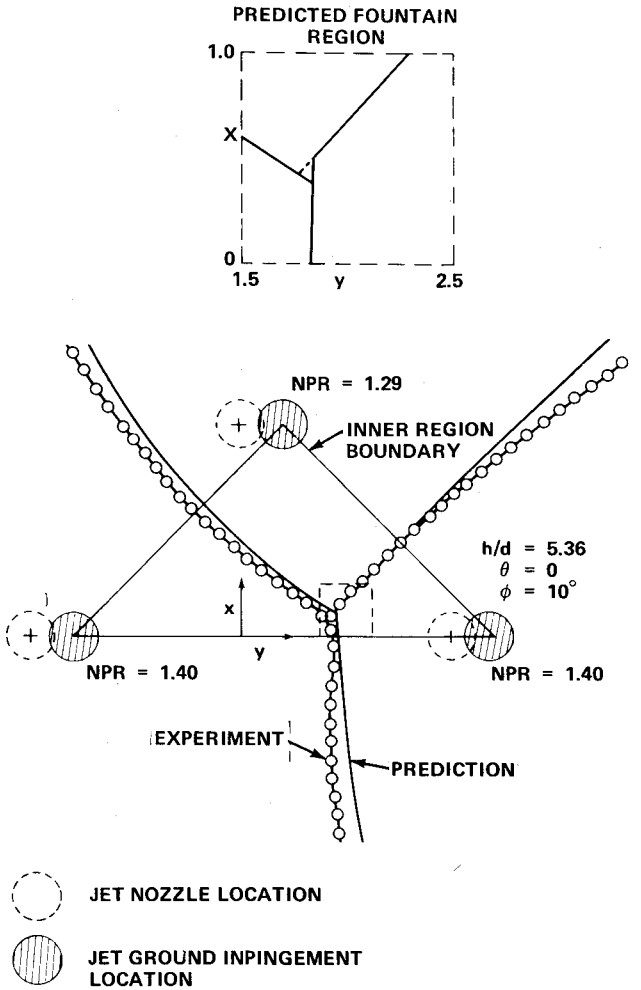

Fig. 14 Asymmetrical stagnation line prediction vs experiment.

Additional flow visualization experiments were conducted with the ground plane rolled about an axis in the plane of symmetry. Figure 12 is a view of ground plane flow for a 10-deg roll attitude and zero pitch. Here, the stagnation line pattern is asymmetric and the fountain has simultaneously shifted away from the plane of symmetry and toward the inner region boundary. This shift in fountain position is illustrated further by Fig. 13, which was obtained by tracing the stagnation lines from half-scale flow visualization photos. The nozzle assembly was initially pitched 2 deg, 40 min at zero roll to cause the stagnation point to move toward jet No. 2. Holding pitch constant, the ground plane was then rolled to 5- and 10-deg angles. This caused the stagnation point to move laterally from the plane of symmetry and away from jet No. 2 toward the inner region boundary. Apparently, roll attitude causes a change in momentum balance favoring both the lateral and rearward stagnation point movement shown. Other three-jet spacings would result in different stagnation point movements.

Figure 14 shows a comparison between calculated results and experiment for the 0-deg pitch, 10-deg roll case. Fountain location at the ground plane is determined analytically by the mutual intersection point of three stagnation lines. For an asymmetric ground flow pattern, the three predicted stagnation lines do no exhibit a mutual intersection point. This is due to the dissimilar curvature of the three stagnation lines. A triangular intersection region results, as shown in the inset on Fig. 14. Since the physical flow cannot sustain all three sides of the triangular region, one side is eliminated. Examination of the intersection region of Figs. 12 and 13 supports this procedure.

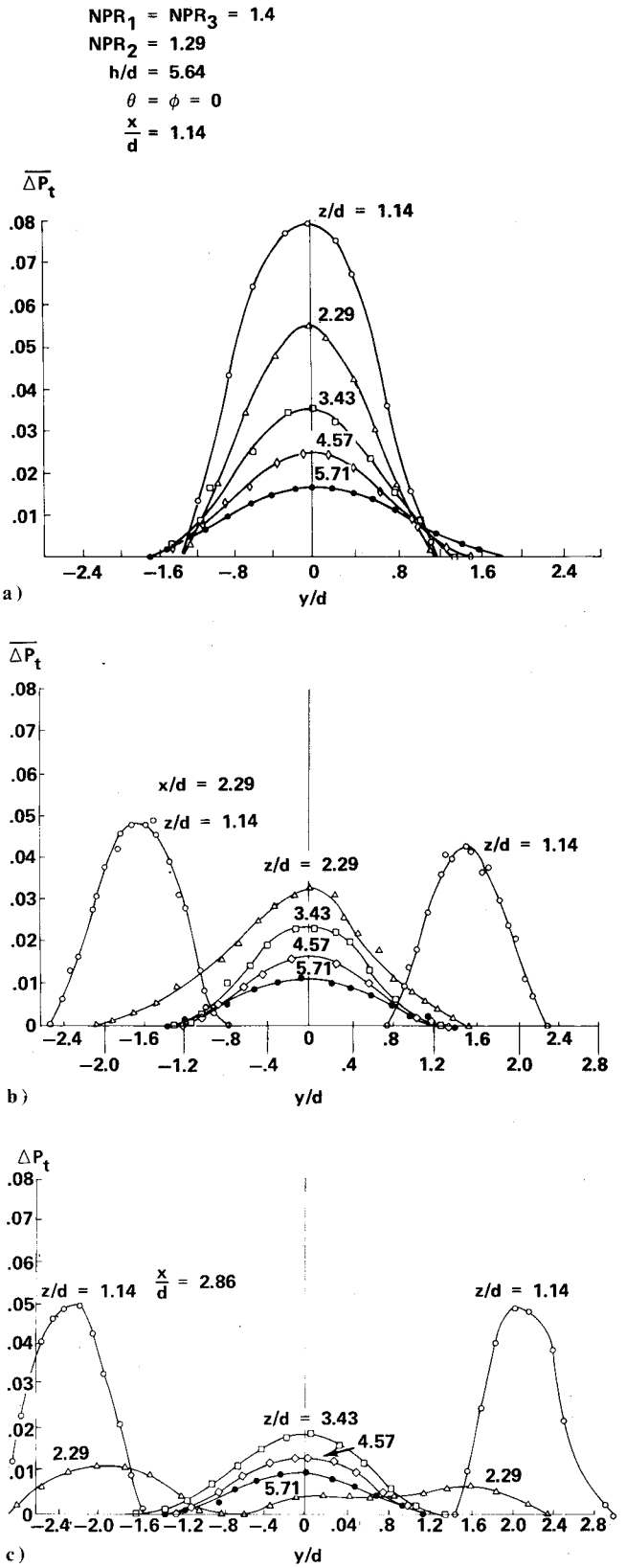

Fig. 15 Fountain and upwash pressure distribution in the inner region of three jets, vertical impingement.

Fountain Formation

Total pressure surveys of the three-jet configuration are shown in Fig. 15. The survey plane represented by $X/d = 1.14$ is through a significant part of the fountain region. The next survey plane at $X/d = 2.29$ shows the formation of two distinct upwash peaks at the lowest height. At the next height

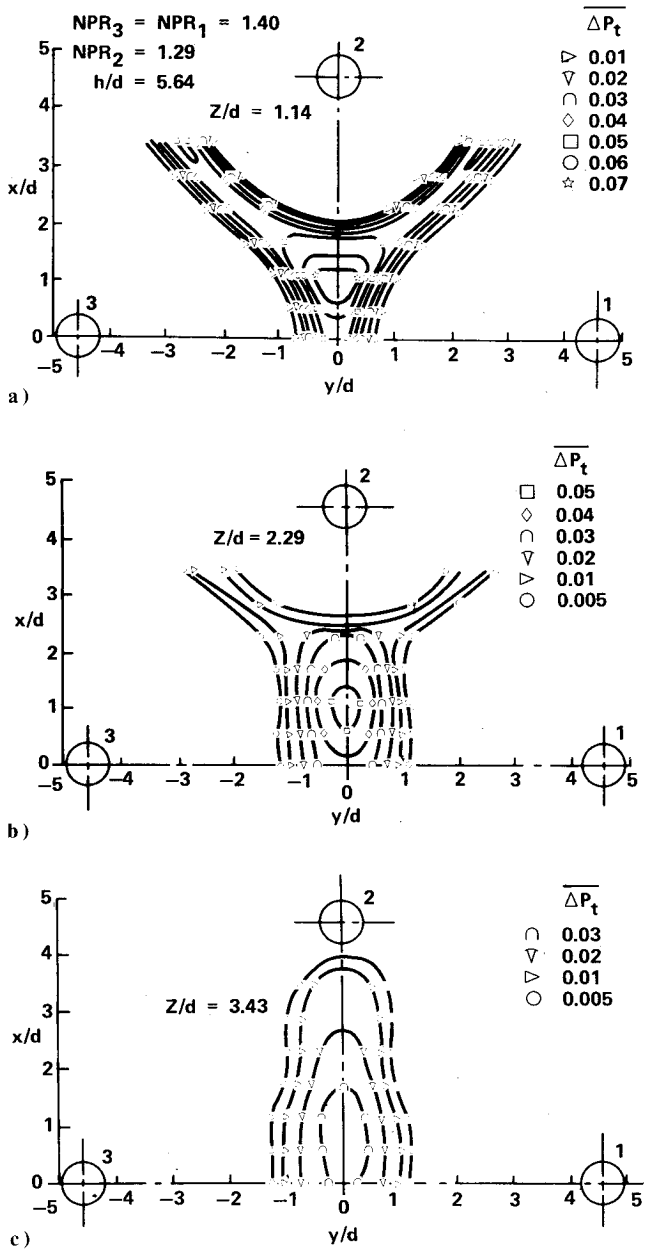

Fig. 16 Isopressure distribution in the fountain and upwash regions of three jets, vertical impingement.

measured ($Z/d=2.29$), only one central pressure peak is present. This traverse shows the rapid formation of a central fountain from the two forward upwash regions. The third survey plane at $Z/d=2.86$ shows the development of two forward branch upwash regions and the rapid weakening of the fountain region.

Figure 16 shows the isopressure patterns of the upwash and fountain flow measured at several heights above ground. At $Z/d=1.14$, the upwash pattern of each individual jet pair is easily distinguishable. A small central fountain region is starting to form due to the coalescence of individual upwash flows. It is interesting to note that the fountain flow is reinforced due to the coalescence of the individual upwash flows. This is exhibited by the maximum total pressure value of the fountain region, which exceeds peak pressure values between individual jet pairs. At $Z/d=2.29$, the individual upwash flow from lateral jet pairs is barely distinguishable

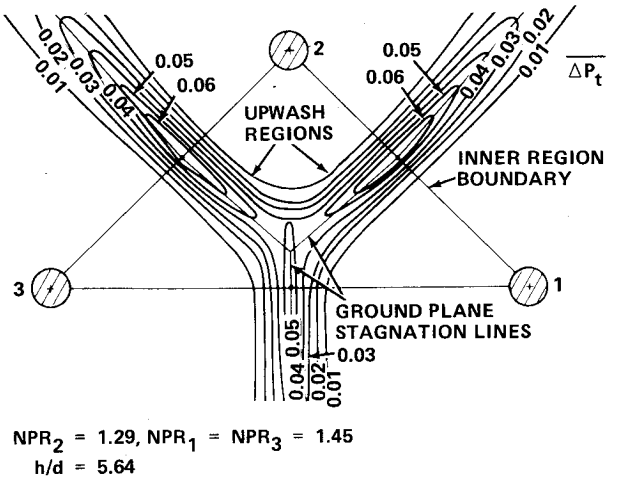

Fig. 17 Numerically simulated isopressure pattern of a three-jet group, $Z/d=1.14$.

with a strong central fountain region almost completely dominating. At $Z/d=3.43$, the central fountain is completely formed and the individual upwash flows have coalesced.

An isopressure pattern similar to Fig. 16 was calculated for comparison and is shown in Fig. 17. The calculated pattern represents the upwash just before coalescence of individual jet pairs and, as a result, does not show the development of a central fountain region with its higher pressures. This occurs later at a greater height. In contrast, test results (Fig. 16) show the initial stage of fountain development already occurring.

Conclusions

Detailed flowfield pressure measurements have been made in the upwash and fountain regions of two- and three-jet arrangements. In addition, both ground plane and vertical plane of symmetry flow visualization techniques have been used to identify the complex nature of multijet flowfields. The position of ground plane stagnation lines is apparently affected by the formation of vortices between the jet impingement region and the fountain or upwash. One can infer that the relative strength of these vortices is affected by ground inclination, where the strongest vortex will form on the "downhill" side of the upwash in closest proximity to an impinging jet.

Real fluid effects such as the formation of vortices, the entrainment of surrounding air by the fountain and the reinforcement of fountain pressures have not as yet been modeled by the available methodology. Empirical factors allow present methods to achieve a reasonable degree of accuracy despite the aforementioned limitations. The need for additional, carefully structured tests is evident. Future methodology improvements will depend on comprehensive tests to understand and model the multijet flowfield.

References

[1] Siclari, M. J., Hill, W. G. Jr., and Jenkins, R. C., "Investigation of Stagnation Line and Upwash Formation," AIAA Paper 77-615, Palo Alto, Calif., June 6-8. 1977.

[2] Siclari, M. J., Aidala, P., Wohllebe, F., and Palcza, J. L., "Development of Prediction Techniques for Multi-jet Thermal Ground Flowfield and Fountain Formation," AIAA Paper 77-616, Palo Alto, Calif., June 6-8, 1977.

[3] Kotansky, D. R., Durando, N. A., Bristow, D. R., and Saunders, P. W., "Multi-Jet Induced Forces and Moments on VTOL Aircraft Hovering In and Out of Ground Effect," Naval Air Development Center, Rept. No. NADC-77-229-30, June 1977.